

¹H NMR, Surface Tension, Viscosity, and Volume Evidence of Micelle–Polymer Hydrophobic Interactions: LiPFN–PVP System[†]

Bianca Sesta,^{*,‡} Anna Laura Segre,[§] Alessandro D'Aprano,[‡] and Noemi Proietti[‡]

Dipartimento di Chimica, Università La Sapienza, P.le A. Moro 5, 00185 Roma, Italy, and Area di Ricerca CNR di Roma, Servizio NMR, Via Salaria km 29.3, Montelibretti, Italy

Received: May 13, 1996; In Final Form: October 8, 1996[©]

Proton NMR investigations on lithium heptadecafluorononanoate, LiPFN, in poly(vinylpyrrolidone), PVP, aqueous solutions have been carried out. NMR spectra reveal that the amphiphile, in its micellar form, links to the polymer chains by hydrophobic interactions with the pyrrolidone functional group of the polymer, causing a significant change in the PVP structure. Surface tension, viscosity, and volume measurements on LiPFN–PVP–water systems support the NMR evidence.

I. Introduction

Interactions between polymers and surfactants are of considerable recent interest.^{1–6} Both compounds, under the physical and chemical influence of the environment, can assume supramolecular structures (*i.e.* micelle assemblies, or much more complex structures like liquid crystalline mesophases, for the surfactants^{7–8} and conformation changes, to give tertiary structures, for the polymers^{9,10}).

The supramolecular structures of the amphiphiles, as well as the stable conformations of polymers, obey the thermodynamic requirements of stability imposed by the inter- and intramolecular forces. The simultaneous presence of the surfactant molecules and of the polymer in aqueous solution leads to new and different equilibria controlled by the mutual interaction of the functional groups of these substances. Structural aspects of such mixed systems, although the object of many studies,^{11–14} have not yet been completely clarified.

Surfactant–polymer mixtures constitute an attractive subject of research also from a technological point of view. It has been found that many adhesion processes of polymers on metal,¹⁵ silica,^{16–17} and other surfaces,^{18–19} are often made easier in the presence of suitable surfactants.

Among anionic surfactants, alkyl sulfates and in particular sodium dodecyl sulfate, SDS, have been widely used in mixtures with synthetic polymers, like poly(vinylpyrrolidone), PVP, or poly(ethyleneoxide), PEO.^{20–23} In this paper the research will be extended to the perfluorinated salts.

These compounds are a typical class of surfactants in which all hydrogen atoms of the hydrocarbon moiety have been replaced with fluorine atoms. Despite their high cost, these amphiphilic substances have been widely employed for particular purposes. Added to some types of cement, they reduce the shrinkage and the cement becomes much more resistant to weather.¹⁵ Metal surfaces, treated with Zonyl products (containing fluorinated surfactants), acquire water and solvent repellency. They also prevent corrosion damage, as well as acid and/or alkali attack.^{24–25}

A fundamental difference exists in the chemical properties of hydrocarbon and perfluorinated surfactants. Hydrocarbon

salts are, in fact, soluble in aqueous media and highly soluble in organic solvents, while perfluorinated salts are hydrophobic as well as oleophobic. Fluorinated surfactants may be used in solvent-based adhesive or in water-based adhesive since they increase the wetting and the penetration process of several substrata on steel or plastic surfaces.¹⁵

Despite their wide practical use, physicochemical studies on perfluorosurfactants are quite limited. The micellization process of lithium perfluorononanoate in aqueous solution has been investigated by some of us.²⁶

The present study is based on surface tension, viscosity, volume, and ¹H NMR measurements carried out on 1% PVP aqueous solutions to which increasing amounts of lithium perfluorononanoate, LiPFN, have been added. Since LiPFN does not have hydrogens in its molecule, ¹H NMR constitutes a method particularly suitable to point out the variations in the polymer structure.

The change of the chemical physics properties of PVP in the presence of some surfactant, in particular of sodium dodecyl sulfate, SDS, has been previously investigated by other authors.²⁰ Since SDS and LiPFN have very close values of the critical micellar concentration, cmc, a comparative analysis of the differences and/or of the analogies between PVP–SDS and PVP–LiPFN systems should give useful information for a better knowledge of the surfactant–polymer mechanism of interaction.

II. Experimental Section

A. Materials. Poly(vinylpyrrolidone), PVP (average molecular weight 360×10^3), was used as received from Fluka. Sodium dodecyl sulfate, SDS (Sigma), was twice dissolved in water and precipitated by adding acetone (C. Erba high purity grade product). Lithium perfluorononanoate, LiPFN, was synthesized by dissolving heptadecafluorononanoic acid (Aldrich) in ethanol and neutralizing with lithium hydroxide, in aqueous solution. The end point of titration was determined using phenolphthalein as indicator. The alcohol was removed by heating and the solution was freeze-dried. The salt was then purified by solubilization in acetone and precipitation with chloroform (high purity grade product from C. Erba). The final product was vacuum dried at 80 °C for 3 days. Molecular structures of PVP and LiPFN are shown in Figures 1.

Bidistilled water, with very low specific conductance, $\chi_0 = 2 \times 10^{-7} \Omega \text{ cm}^{-1}$, was used to prepare the solutions. Samples to be measured by NMR have been prepared using deuterium oxide (Merck, 99.8%).

* Corresponding author.

[†] Results presented in this paper will be included in the thesis to be presented by Noemi Proietti as required for partial fulfillment of requirements for the degree of "Dottore di Ricerca in Scienze Chimiche", University of Rome "La Sapienza".

[‡] Università La Sapienza.

[§] Area di Ricerca CNR di Roma, Servizio NMR.

[©] Abstract published in *Advance ACS Abstracts*, December 15, 1996.

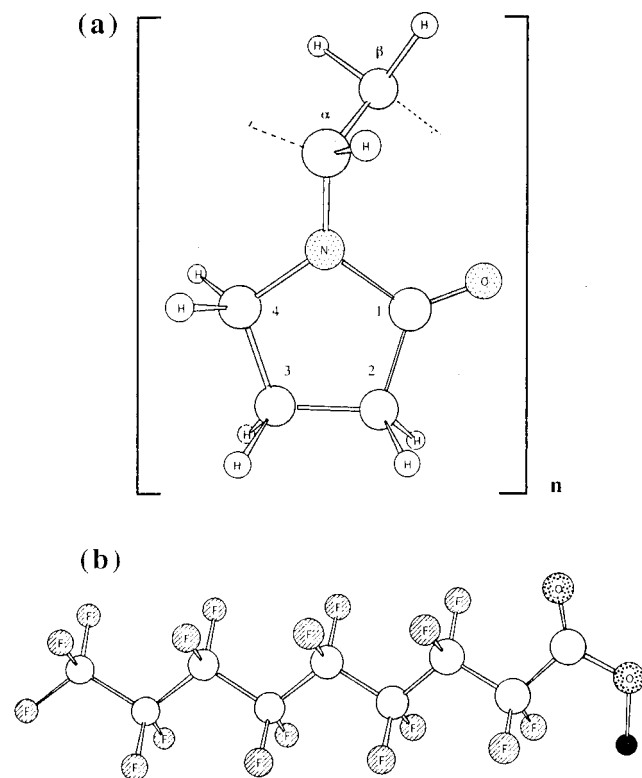


Figure 1. Molecular structure of the monomeric unity of PVP (a) and LiPFN (b).

TABLE 1: Physical Properties of Solvents at 25 °C

solvent	d (g cm ⁻³)	η (cP)	γ (dyn cm ⁻¹)
water	0.997 06	0.8903	71.9
water+PVP(1%)	0.999 23	2.7685	66.8

B. Procedures and Apparatus. All the solutions were prepared by weight. Experimental runs were carried out by adding concentrated master solutions of surfactant to the solvent. For the ternary systems, a mixture of water + PVP (1%) was used as solvent and to prepare the master solution of surfactant. Table 1 summarizes the physical properties of the solvents, measured with the apparatus described below.

¹H NMR spectra have been obtained with a Bruker AMX 600 operating at 600.13 MHz. The concentration of PVP in D₂O was kept constant (1% w/w) while variable amounts of surfactant (from 10⁻⁶ to 10⁻¹ mol kg⁻¹) were added. Residual HOD signal was not suppressed. A 90° pulse (~10–11 μs) was followed by a delay of 2 s with an acquisition time of 2.2 s, thus ensuring the full relaxation of the system. The time domain was 32K points, followed by a Fourier transformation of 16K points without any lines broadening or enhancement function.

The surface tensions, γ , were measured by the ring method, with an accuracy of ± 0.1 dyn cm⁻¹. A computerized Lauda digital tensiometer, provided with an automatic device to select the rising velocity of the platinum ring and to set the time between two measurements, was used. The temperature was maintained at 25.00 ± 0.01 °C by pumping water from an outside cryogenic bath (Heto DTB-CB6) into a double-walled jacket surrounding the circular vessel containing about 10–12 cm³ of solution. The tensiometer was calibrated with water and acetone.²⁷

The densities were measured at 25 ± 0.002 °C by an A. Paar (Model 602) vibrating tube densimeter. The thermal stability was assured by a temperature controller (CBII-DTB from Heto)

and checked with a F 25 precision digital thermometer from Automatic System Laboratories.

The measured frequencies, τ , were converted into densities, d , by the equation

$$d = (\tau^2 - B)/A \quad (1)$$

The instrument constants A and B were determined using water and acetone as calibrating liquids.²⁷

The viscosities were measured by an Ubbelohde viscometer, with long flow times to avoid kinetic energy correction, dipped in a thermostatic bath at 25 ± 0.01 °C. The measurements were repeated five or more times, until successive determinations agreed to within ± 0.1 s.

III. Results and Analysis

¹H NMR spectra for 1% PVP aqueous solution and for LiPFN–water–PVP systems, containing different amounts of surfactant, are shown in Figure 2.

The surface tension data, γ , and the corresponding surfactant molal concentrations, m , for LiPFN and SDS in pure water and in 1% PVP aqueous solutions are summarized in Table 2. The surface tension results of SDS–water and SDS–water–PVP systems are in full agreement with those previously reported.^{20,28–29}

The experimental trends of γ vs $\ln m$ in pure water are shown in curves *a* of Figures 3 and 4. The breakpoints in these curves are indicative of the critical micelle concentration (cmc).

The tensiometric data below the cmc have been analyzed by the Gibbs adsorption isotherm³⁰

$$-d\gamma = \sum [n_i^\sigma / A] d\mu_i = \sum \Gamma_i d\mu_i \quad (2)$$

where A is the surface area per molecule, μ_i and n_i^σ are the chemical potential and the number of moles in the surface of the components i , respectively, and Γ_i is the surface concentration (*the surface excess*) of the components i .

For binary system, eq 2 can be set as

$$-d\gamma = \Gamma_1 d\mu_1 + \Gamma_2 d\mu_2 \quad (3)$$

If the reference plane, which ideally divides the bulk and surface regions, is set so that $\Gamma_1 = 0$,³¹ eq 3 can be simplified as

$$d\gamma = -\Gamma_2 d\mu_2 \quad (4)$$

Differentiating the chemical potential (expressed in terms of the solute activity, a_2), eq 4, at constant temperature, becomes

$$d\gamma = -\Gamma_2 RT d \ln a_2 \quad (5)$$

which for 1:1 electrolytes must be rewritten³² as

$$d\gamma = -2\Gamma_2 RT d \ln a_2 \quad (6)$$

For very diluted solutions, setting $a_2 \approx m$, we obtain

$$\Gamma_2 = -d\gamma / (2RT d \ln a_2) \approx -d\gamma / (2RT d \ln m) \quad (7)$$

Near the cmc, Γ_2 assumes its maximum value, Γ_{\max} , from which the minimum area (in Å²) per molecule of surfactant,

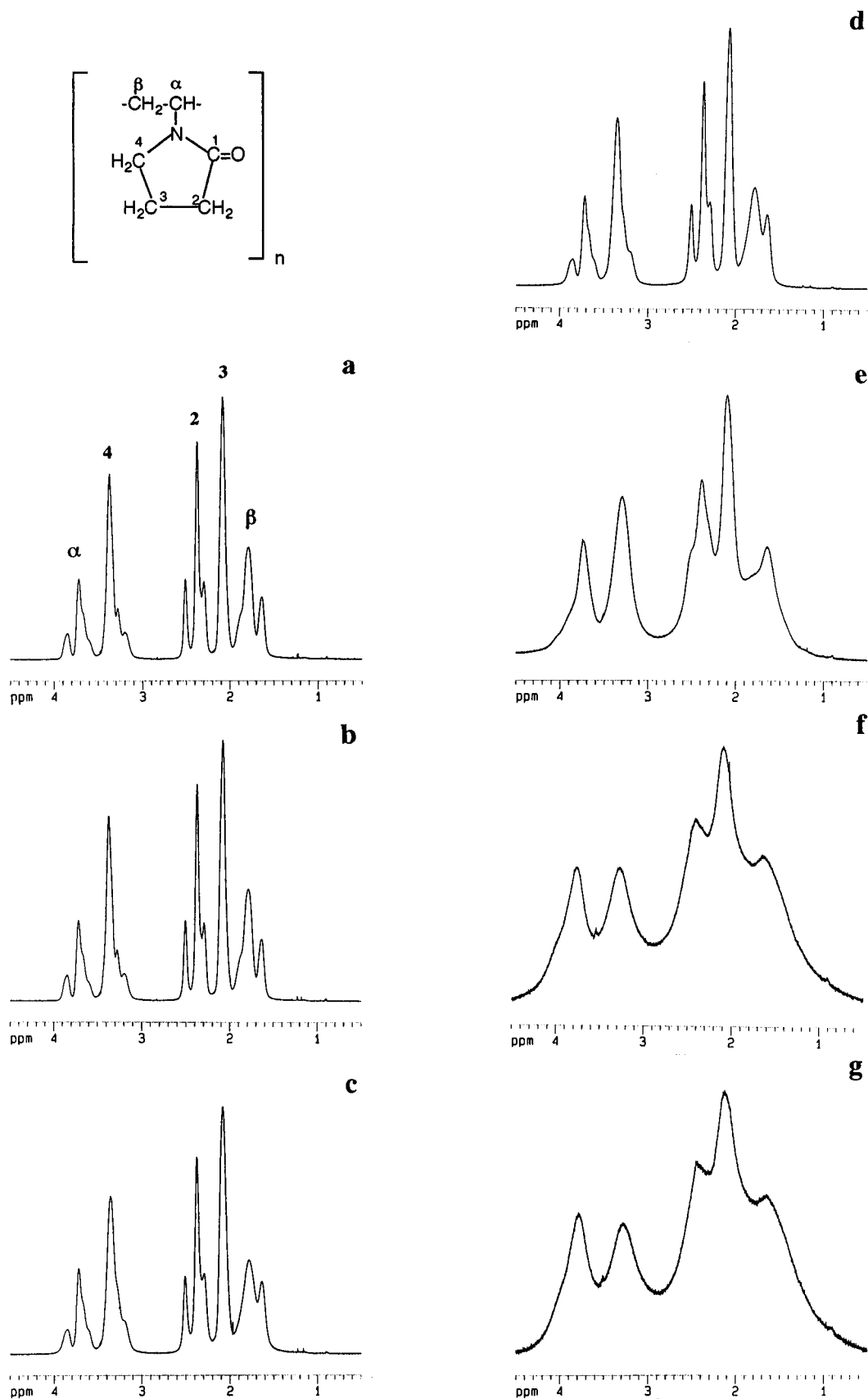


Figure 2. ^1H NMR resonances of PVP in D_2O at different LiPFN molal concentration, m : (a) $m = 0$; (b) $m = 1.4 \times 10^{-4}$; (c) $m = 1.2 \times 10^{-3}$; (d) $m = 3.6 \times 10^{-3}$; (e) $m = 2.0 \times 10^{-2}$; (f) 9.1×10^{-2} ; (g) 2.1×10^{-1} (spectrum amplified 10 times).

A_{\min} , required by the surfactant head group can be calculated as

$$A_{\min} = 10^{14}/(N\Gamma_{\max}) \quad (8)$$

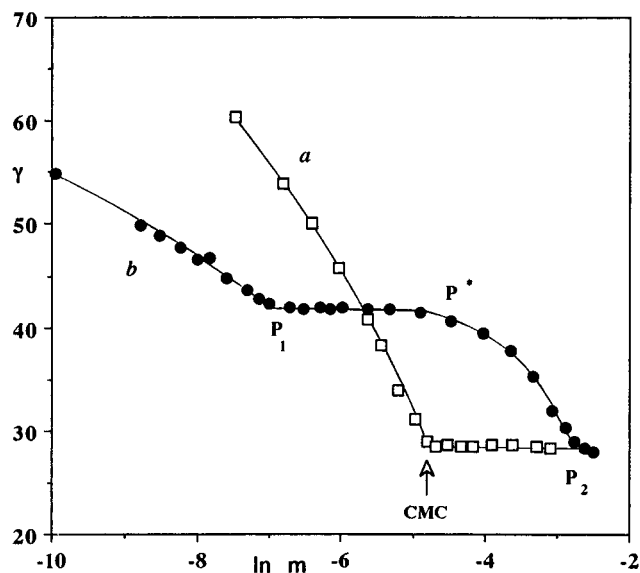
where N is the Avogadro number.

The critical micelle concentration and the surface tension properties of LiPFN and SDS in water are listed in Table 3.

The curves b of Figures 3 and 4 show the experimental behaviors of γ vs $\ln m$ for LiPFN and SDS in water + PVP (1%). As can be seen, in the presence of the polymer, the $\gamma =$

TABLE 2: Molalities, m , and Surface Tensions, γ , of LiPFN and SDS in Water and in PVP(1%) Aqueous Solution at 25 °C

LiPFN				SDS			
water		water +PVP(1%)		water		water+PVP(1%)	
1000 <i>m</i> mol kg ⁻¹	γ (dyn cm ⁻¹)	1000 <i>m</i> (mol kg ⁻¹)	γ (dyn cm ⁻¹)	1000 <i>m</i> (mol kg ⁻¹)	γ (dyn cm ⁻¹)	1000 <i>m</i> (mol kg ⁻¹)	γ (dyn cm ⁻¹)
0.562 72	60.3	0.048 000	54.9	0.647 59	68.4	0.867 80	53.0
1.0807	53.9	0.151 90	49.9	1.6331	61.5	1.5837	51.4
1.6406	50.0	0.197 30	48.9	3.1351	54.7	1.7259	51.0
2.3831	45.8	0.263 20	47.7	4.6548	49.0	2.6421	48.5
3.5975	40.8	0.334 70	46.6	6.3600	45.0	2.8828	47.9
4.3421	38.2	0.398 60	46.7	7.8066	41.1	3.7092	48.0
5.4352	34.0	0.504 80	44.7	9.3796	39.0	3.7529	47.0
6.9044	31.2	0.670 90	43.6	10.762	39.3	4.5837	47.0
8.1704	28.9	0.791 30	42.8	12.308	39.9	5.4402	47.3
9.2757	28.5	0.909 40	42.2	14.494	39.9	6.2431	47.0
11.059	28.6	1.2012	42.0	17.029	39.8	7.0498	46.9
13.148	28.5	1.4464	41.8	19.681	39.8	7.1743	47.5
15.753	28.5	1.8429	42.0			7.6551	47.0
20.287	28.7	2.1138	41.8			8.7197	47.0
26.772	28.7	2.5230	42.0			9.7704	46.7
37.244	28.5	3.5747	41.7			10.730	46.0
45.322	28.3	4.8395	41.7			11.891	45.7
		7.3845	41.4			12.833	45.3
		11.348	40.6			13.981	44.9
		17.844	39.5			15.548	44.1
		26.053	37.8			17.911	43.3
		35.929	35.2			20.602	42.8
		46.681	32.0			23.569	41.6
		55.662	30.3			26.969	40.6
		63.691	29.0			30.912	40.1
		73.530	28.3			35.778	40.0
		82.860	28.0				
		28.0					

**Figure 3.** Surface tension γ (dyn cm⁻¹) of LiPFN in water (curve *a*) and in PVP(1%) aqueous solution (curve *b*) against the natural logarithm of surfactant molality, $\ln m$, at 25 °C.

$f(\ln m)$ functions assume a trend much more complex than in pure water. In particular, both systems show two break points, P_1 and P_2 , indicating the concentrations where transition points of the systems occur.¹

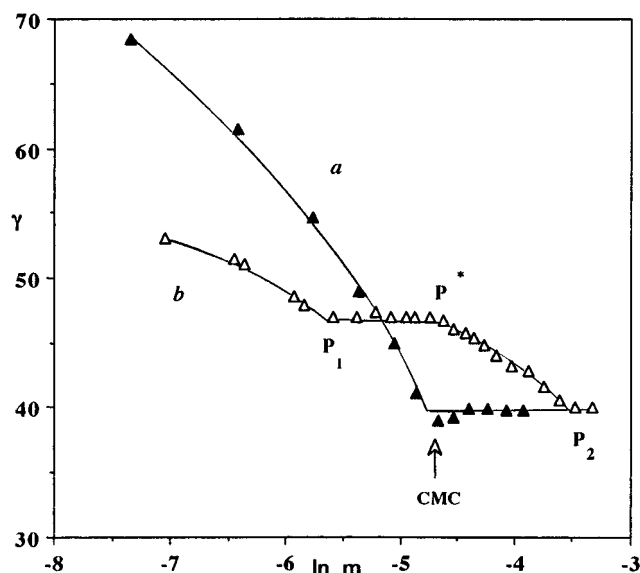
For the ternary systems surfactant–polymer–water, the Gibbs isotherm becomes

$$-d\gamma = \Gamma_1 d\mu_1 + \Gamma_2 d\mu_2 + \Gamma_3 d\mu_3 \quad (9)$$

As the polymer concentration is constant, we can assume³

$$\Gamma_1 d\mu_1 + \Gamma_3 d\mu_3 = 0 \quad (10)$$

where Γ_1 and Γ_3 refer to water and polymer surface excesses.

**Figure 4.** Surface tension γ (dyn cm⁻¹) of SDS in water (curve *a*) and in PVP(1%) aqueous solution (curve *b*) against the natural logarithm of surfactant molality, $\ln m$, at 25 °C.**TABLE 3: Surface Tension Properties of LiPFN and SDS in Water at 25 °C**

	cmc (mol kg ⁻¹)	$10^{10}\Gamma_{\max}$ (mol cm ⁻²)	A_{\min} (Å ²)
LiPFN	8.2×10^{-3}	2.7×10^{-3}	62
SDS	8.4×10^{-3}	3.0×10^{-3}	56

Thus, even for the ternary systems, the surface tension data can be analyzed with eqs 7 and 8.

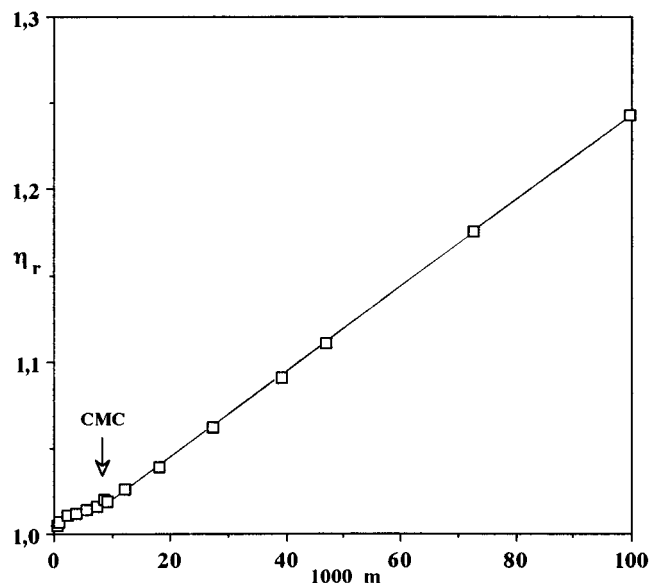
The surface areas per head group, $A_1(P_1)$ and $A_2(P_2)$ for LiPFN and SDS in water + PVP(1%), calculated from the slopes of curves *b* of Figures 3 and 4, just below the first and the second

TABLE 4: Surface Tension Properties of LiPFN and SDS in Water+PVP(1%) at 25 °C

	P_1 (mol kg ⁻¹)	$(A_1)P_1$ (Å ²)	P_2 (mol kg ⁻¹)	$(A_2)P_2$ (Å ²)
LiPFN	0.9×10^{-3}	191	73×10^{-3}	76
SDS	2.8×10^{-3}	183	31×10^{-3}	142

TABLE 5: Molalities, m , and Relative Viscosities, η_r , of LiPFN in Water; Molalities, m , Relative Viscosities, η_r , Densities, d , and Apparent Molal Volumes, Φ_v , of LiPFN in Water+PVP(1%) at 25 °C

water		water+PVP(1%)			
1000 <i>m</i> (mol kg ⁻¹)	η_r	1000 <i>m</i> (mol kg ⁻¹)	η_r	d (g cm ⁻³)	(Φ_v) (cm ³ mol ⁻¹)
0.0000	1.0000	0.0000	1.0000	0.999 23	
0.5830	1.0048	0.5768	0.9994	0.999 37	227.2
0.9770	1.0073	0.9036	1.0010	0.999 47	226.5
2.4970	1.0112	1.5880	1.0319	0.999 62	224.3
3.8500	1.0115	3.7670	1.2223	1.000 14	228.2
5.6810	1.0143	5.6720	1.3601	1.000 58	231.7
7.3220	1.0159	6.9730	1.4584	1.000 88	233.0
8.6970	1.0198	8.2760	1.5104	1.001 16	236.3
9.2200	1.0188	10.618	1.6301	1.001 69	237.7
12.313	1.0254	15.817	1.8107	1.002 88	238.4
18.049	1.0386	26.247	2.0421	1.005 35	235.4
27.221	1.0621	35.966	2.0510	1.007 62	234.8
39.178	1.0910	46.673	2.1425	1.010 07	235.2
46.765	1.1108	59.343	2.2357	1.012 98	235.1
72.742	1.1758	71.886	2.2037	1.015 68	237.3
99.654	1.2429	84.049	2.1453	1.018 52	236.0
		98.232	2.1518	1.021 65	236.5

**Figure 5.** Relative viscosity, η_r , of LiPFN in water, against the surfactant molality m , at 25 °C.

transition point, are summarized in Table 4 together with the surfactant concentrations P_1 and P_2 .

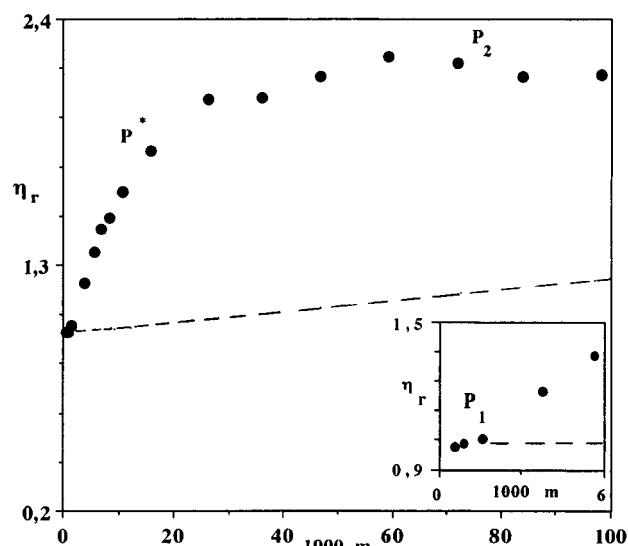
Relative viscosities, η_r , are shown in Table 5. The η_r values, obtained for LiPFN in pure water, are in good agreement with our previous findings.²⁶

As may be seen in Figure 5, the relative viscosities for LiPFN–water systems, as expected, smoothly increase at very low surfactant concentration up to cmc and thereafter increase much more rapidly.

Above the cmc the LiPFN data in water have been fitted by the equation

$$\eta_r = 1 + K\Phi \quad (11)$$

where Φ is the volume fraction solute/solvent and K is a constant

**Figure 6.** Relative viscosity, η_r , of LiPFN in 1% PVP aqueous solution against the surfactant molality m , at 25 °C. The dashed curve concerns the viscosity of the same surfactant in pure water. The inset refers to the viscosity trend of LiPFN in 1% PVP, at high dilution.

which in our case has been found equal to 10, 4 times greater than the values of ~ 2.5 suggested by Einstein for spherical noninteracting solutes. Such a discrepancy depends on several causes, first of all on the increase of the viscous friction when the surfactant is in the micellar form.

The viscosity trend of the LiPFN–PVP(1%)–water system, as a function of surfactant concentration, is shown in Figure 6. An inspection of the figure shows that, starting from a concentration lower than the cmc, the viscosity increases up to a maximum and thereafter it remains approximately constant.

Apparent molal volumes, Φ_v , of LiPFN in water + PVP have been calculated from density data, using the usual equation:

$$\Phi_v = [(d_0 - d)1000]/dd_0m + M_r/d \quad (12)$$

where d and d_0 are the densities of the solution and of the solvent, respectively, M_r is the molecular weight of solute, and m is the molal concentration of the solution.

The results at each molal concentration of LiPFN are summarized in the last column of Table 5. The trend of the $\Phi_v(m)$ function is shown in Figure 7. The minimum in the Φ_v function occurs at the concentration where the first transition point, P_1 , has been observed in the surface tension plot (see curve b of Figure 3).

IV. Discussion

To establish the effects of LiPFN on PVP structure, let us discuss the results obtained with the different techniques used in the present work.

Figure 2a shows the protonic NMR spectrum of the aqueous solution of PVP without LiPFN. In the figure, each resonance peak has been assigned to the functional groups of the polymer.³³ The broadening and splitting of the two peaks of resonances in the $^1\text{H}(\text{C}\alpha)$ and $^1\text{H}_2(\text{C}\beta)$ regions are due to the presence of meso–meso, meso–racemic, and racemic–racemic triads of the polymer.³⁴ The strongest peaks, of these regions, are due to a slightly larger amount of syndiotactic sequences.

At very high dilution, up to $m \approx 0.9 \times 10^{-3}$ of LiPFN, no change in the NMR spectrum was observed (Figure 2b). In the same concentration range, according to the theoretical prediction,³⁰ the surface tension of LiPFN–PVP aqueous solutions (see curve b of Figure 3) regularly decreases by increasing

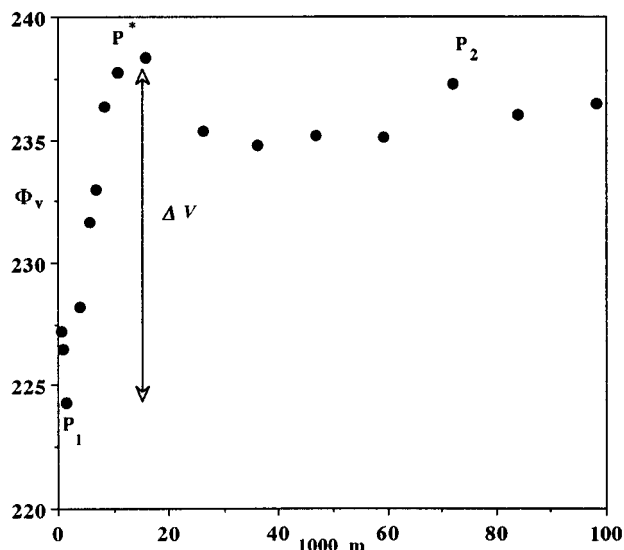


Figure 7. Apparent molal volume, Φ_v (cm³ mol⁻¹), of LiPFN in water + PVP (1%) as a function of the surfactant molality m , at 25 °C.

the surfactant concentration, thus indicating that, below $m \approx 0.9 \times 10^{-3}$, the surfactant is in its molecular state. Comparing curves *b* and *a* of Figure 3, we note that, in the presence of PVP, the surface tension is noticeably lower than in the binary LiPFN–water systems. This phenomenon can be reasonably assigned to the hydrophobic contribution of the polymer to the surface composition. PVP is, in fact, a moderate surface tension agent, the 1% PVP–water solution has $\gamma_0 = 66.8$ dyn cm⁻¹ and pure water $\gamma_0 = 71.9$ dyn cm⁻¹ (Table 1). Furthermore, the slope of the LiPFN–PVP tensiometric plot is appreciably lower than that of LiPFN–water. As a consequence, the area per head group in water, close to its minimum value $A \approx 62$ Å², increases up to 191 Å² in water + PVP, because of the presence of the polymer molecules in the surface monolayer.

As shown in the inset of Figure 6, up to $m \approx 0.9 \times 10^{-3}$ of LiPFN, the relative viscosities of the LiPFN–water–PVP(1%) system show a smooth increase with increasing the surfactant concentration. In the same LiPFN concentration range, the apparent molal volumes regularly decrease (see Figure 7), because of the structure-making effects of the PFN⁻ anion with the surrounding water molecules.³⁵

We consider next the features of the phenomenological curves at and slightly above $P_1 \approx 0.9 \times 10^{-3}$. As concerns the NMR spectra, the proton resonances belonging to ¹H₂(C₃) and ¹H₂(C₄) of the pyrrolidone ring show an appreciable broadening (Figure 2c,d). This phenomenon is better underlined in Figure 8, where the broadening of the resonance peak associated with the ¹H₂(C₄) group is reported as a function of the surfactant concentration. Above P_1 , the surface tension of the LiPFN solutions in 1% PVP remains practically constant at $\gamma \approx 41$ dyn cm⁻¹ over a wide range of surfactant concentrations, P_1 – P^* (curve *b* of Figure 3), as generally occurs when the air–water interface becomes saturated with solute molecules. In the concentration range P_1 – P^* , the viscosity dramatically increases with increasing LiPFN molality. In fact, the viscosity constant, $K = 10$, in water increases to $K = 300$ in the PVP–water system.

All this evidence indicates an interaction process between the surfactant and the polymer. On the basis of the NMR results it can be suggested that, between P_1 and P^* , the ¹H₂(C₃) and ¹H₂(C₄) of the pyrrolidone are mainly responsible for the hydrophobic interactions with perfluorinated anions.

The polymer–surfactant linkage seems to occur when the amphiphile is in its aggregated state. In fact, the linking process

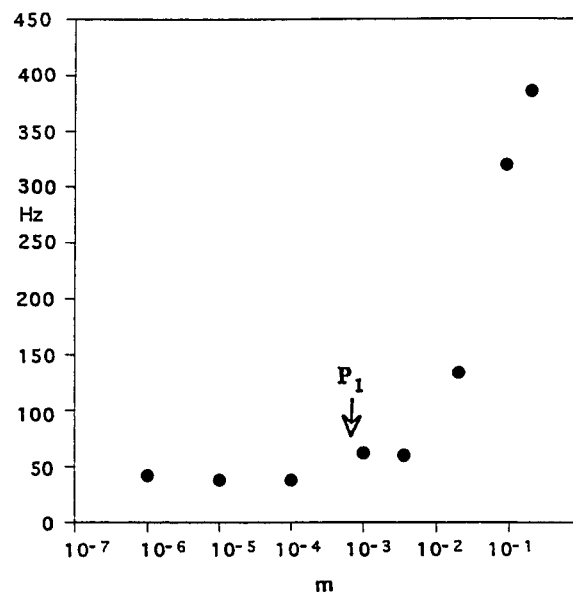


Figure 8. Broadening of the resonance peak related to the ¹H₂(C₄) group as a function of the surfactant concentration.

starts only when a suitable number of perfluorinated molecules are present. The micellization process is well pointed out in the volumetric curve (Figure 7) by an abrupt increase of Φ_v , approximately 14 cm³ mol⁻¹, which is a typical phenomenon occurring during the micellization of most surfactants.^{36–37}

At $P^* \approx 1.1 \times 10^{-2}$ mol kg⁻¹ it could be hypothesized that the polymer becomes saturated with the surfactant aggregates. The inflection of the $\Phi_v(m)$ function at P^* seems to support such a hypothesis.

Above P^* , NMR resonances belonging to the polymer backbone become much more broad as a consequence of the loss of freedom and also of the stiffening of the chains, particularly observable on β groups. Hence at this stage, the whole structure of the polymer is deeply modified (Figure 2e). The surface tension trend also shows significant changes. In fact γ values of curve *b* in Figure 3 decrease as the LiPFN concentration increases, approaching $\gamma = 28$ dyn cm⁻¹ at the second transition point of the ternary system, $P_2 = 7.3 \times 10^{-2}$ mol kg⁻¹. Near P_2 , the area per molecule of the surfactant is $A_2 \approx 76$ Å², a value close to that of LiPFN in pure water (see Table 3). Such a finding seems to indicate that, close to P_2 , some of the PVP molecules leave the water–air interface and move into the bulk.

From P^* to P_2 the function $\eta_r(m)$ reaches a maximum and thereafter slowly decreases (Figure 6), because of the structural changes of the polymer. As known, PVP is an almost atactic polymer. It assumes a quite globular structure in pure water. Under the influence of the linked molecules of surfactant, part of the polymer freedom is lost and a stiffening of the chains occurs, as indicated by the broad NMR resonance shown in Figure 2e,f. Such structural changes allow the alignment of the molecules, in the sense of the viscosity shear stress, and a consequent lowering of the viscosity. The strong broadening of NMR resonances, together with the lowering of the viscosities, allows us to rule out the occurrence of the entangling phenomenon.

At the second transition point, P_2 , the surface monolayer is entirely built up by LiPFN molecules. In fact, the surface tension is practically coincident with the value found for LiPFN in pure water, $\gamma = 28$ dyn cm⁻¹.

Further addition of LiPFN molecules to the solution causes only an increase of the number of free micelles. The partial

molal volume, in fact, does not increase. The NMR resonance (Figure 2g) shows a very strong stiffening of the polymer. (The NMR resonances shown in Figure 2g are 10 times amplified with respect to the other spectra).

The behavior of perfluorinated surfactants, in particular LiPFN, is qualitatively similar to that of many hydrocarbon amphiphiles in the presence of nonionic polymers;¹ however, some important differences can be established. As mentioned in the introduction, the perfluorinated surfactants are much more hydrophobic than their hydrocarbon homologues.^{38–40} Their efficiency in lowering the surface tension of water is much higher than that of the hydrocarbon surfactants. Then, we should expect a more pronounced micelle–polymer linkage, due to hydrophobic interactions, in the presence of perfluorinated surfactants than with hydrocarbon amphiphiles. This hypothesis can be verified by comparing curves *b* of Figures 3 and 4. As may be seen, the first transition point, *P*₁, is largely advanced for LiPFN, with respect to the SDS system. Moreover, the saturation with the surfactant, occurring from *P*₁ to *P*^{*}, is much more extended for LiPFN than for SDS.

Acknowledgment. The authors gratefully acknowledge the support of this work by Ministero dell'Università e della Ricerca Scientifica.

References and Notes

- (1) Lindman, B.; Thalberg, K. In *Interactions of Surfactants with Polymers and Proteins*; Goddard, E. D., Ananthapadmanabhan, K. P., Eds.; CRC Press: Boca Raton, FL, 1993; Chapter 5, p 203.
- (2) Thalberg, K.; Lindman, B. *J. Phys. Chem.* **1989**, *93*, 1478.
- (3) Thalberg, K.; Lindman, B.; Karlstrom, G. *J. Phys. Chem.* **1991**, *95*, 3370.
- (4) Zhang, K.; Jonstromer, M.; Lindman, B. *J. Phys. Chem.* **1994**, *98*, 2459.
- (5) Zhang, K.; Jonstromer, M.; Lindman, B. *Colloids Surf. A* **1994**, *87*, 133.
- (6) Moren, A. K.; Khan, A. *Langmuir* **1995**, *11*, 3636.
- (7) Wyn-Jones E.; Gormally, J. *Aggregation Process in Solution*; Elsevier: Amsterdam, 1983.
- (8) Fontell, K. In *Surfactants in Solution*; Mittal, K. L., Lindmann, B., Eds.; Plenum Press: New York, 1984; Vol. I, p 69.
- (9) Doi, M.; Edwards, S. F. *The Theory of Polymer Dynamics*; Clarendon Press: Oxford, U.K., 1986.
- (10) Des Cloiseaux, J.; Jannink, J. *Polymers in Solution: Their Modelling and Structure*; Oxford Science Publishers: Oxford, U.K., 1990.
- (11) Cabane, B. *J. Phys. Chem.* **1977**, *81*, 1639.
- (12) Turro, N. J.; Baretz, B. H.; Kuo P. L. *Macromolecules* **1984**, *17*, 1321.
- (13) Chari, K.; Lenhart, W. C. *J. Colloid Interface Sci.* **1990**, *137*, 204.
- (14) Bjorling, M.; Herslof-Bjorling, A.; Stilbs, P. *Macromolecules* **1995**, *28*, 6970.
- (15) Kissa, E. In *Fluorinated Surfactants: Synthesis, Properties, Applications*; Kissa, E., Ed.; Marcel Dekker Inc.: New York, 1993; Chapter 8, p 325.
- (16) Esumi, K.; Oyama, M. *Langmuir* **1993**, *9*, 2020.
- (17) Maltesh, C.; Somasundaran, P. *J. Colloid Interface Sci.* **1992**, *153*, 301.
- (18) Otsuka, H.; Esumi, K. *Langmuir* **1994**, *10*, 45.
- (19) Otsuka, H.; Esumi, K. *J. Colloid Interface Sci.* **1995**, *170*, 113.
- (20) Arai, H.; Murata, M.; Shinoda, K. *J. Colloid Interface Sci.* **1971**, *37*, 223.
- (21) Murata, M.; Arai, H. *J. Colloid Interface Sci.* **1973**, *44*, 475.
- (22) Jones, M. N. *J. Colloid Interface Sci.* **1967**, *23*, 36.
- (23) Moroi, Y.; Akisada, H.; Saito, M.; Matuura, R. *J. Colloid Interface Sci.* **1977**, *61*, 233.
- (24) Klein, H. G.; Meussdoerffer, J. N.; Niederprum, H. *Metalloberflache* **1975**, *29*, 559.
- (25) Klein, H. G.; Meussdoerffer, J. N.; Niederprum, H.; Wechsberg, M. *Tenside* **1978**, *15*, 2.
- (26) La Mesa, C.; Sesta, B. *J. Phys. Chem.* **1987**, *91*, 1450.
- (27) *Handbook of Chemistry and Physics*; CRC Press: Boca Raton, FL, 1985.
- (28) Knox, W. J.; Parshall, T. O. *J. Colloid Interface Sci.* **1970**, *33*, 16.
- (29) Goddard, E. D.; Hanna, R. B. *J. Am. Oil Chem. Soc.* **1977**, *54*, 561.
- (30) Gibbs, J. W. *Collected Work*; Longmans Green: New York, 1928; Vol. I.
- (31) Evans, D. F.; Wennertrom, H. *The Colloidal Domain*; VCH Publishers, Inc.: New York, 1994; Chapter 2, p 64.
- (32) Couper, A. In *Surfactants*; Tadros, Th. F., Ed.; Academic Press: London, 1984; p 20.
- (33) Sylverstein, R. M.; Bassle, G. C.; Morril, T. C. *Spectrometric Identification of Organic Compounds*; Wiley and Sons: New York, 1981; pp 222–225.
- (34) Borey, F. A. *High Resolution NMR of Macromolecules*; Academic Press: New York, 1972.
- (35) Lalibertè, L. H.; Conway, B. H. *J. Phys. Chem.* **1970**, *74*, 4116.
- (36) De Lisi, R.; Perron, G.; Desnoyers, J. E. *Can. J. Chem.* **1980**, *58*, 959.
- (37) D'Aprano, A.; Sesta, B.; Iammarino, M.; Filippi, C.; Princi, A.; Proietti, N. *Langmuir* **1994**, *10*, 2100.
- (38) Shinoda, K.; Hato, M.; Hayashi, T. *J. Phys. Chem.* **1972**, *76*, 909.
- (39) Handa, T.; Mukerjee, P. *J. Phys. Chem.* **1981**, *85*, 3916.
- (40) Korematsu, K.; Okawauchi, H.; Sugihara, G. *J. Phys. Chem.* **1985**, *89*, 5308.